FEBS Letters 346 (1994) 3–16

FEBS 14098

The Seventh Datta Lecture

Membrane bending energy concept of vesicle- and cell-shapes and shape-transitions

E. Sackmann*

Physics Department (Biophysics Group E22), Technische Universität München, D-85747 Garching, Germany

Received 8 April 1994

Abstract

The main objective of this lecture is to discuss the role of lipid-bilayer elasticity (1) for the self-organization of lipid/protein-bilayers (2) for the stabilization of domain structures and shapes of cell membranes and (3) for the control of shape transitions (e.g. bud- and pit-formation) and shape instabilities (vesicle fission). It is demonstrated that many complex shape transitions of cell membranes can be mimicked by single lipid bilayer vesicles by simply varying the area-to-volume ratio or by chemically induced bending moments suggesting that these processes are governed by the universal minimum bending energy concept of closed shells composed of stratified membranes. The essential role of the coupling between curvature and phase separation in mixed membranes for the formation and stabilization of local pits and buds or the fission of budded vesicles is demonstrated. Finally, we discuss the consequences of the pronounced thermally excited bending undulations of the hyperelastic membranes for the membrane tension, the material exchange at membrane surfaces and the control of the adhesion of vesicles (or cells) on solid substrates.

Key words: Membrane self organization; Vesicle; Lipid protein interaction; Membrane elasticity

1. Introductory remarks

My talk deals with attempts to understand complex membrane processes such as shape transitions of plasma membranes or the vesicle budding and fission from intracellular compartments in terms of universal physical laws which do not depend on the detailed structure of biomembranes.

Fig. 1 shows a cartoon-like image of a plasma membrane. It is a composite type of material made-up of three types of materials: (1) the central lipid/protein bilayer (a two-dimensional smectic liquid crystal), (2) the associated cytoskeleton (a two-dimensional macromolecular network) and (3) the glycocalix (a grafted macromolecular layer).

By coupling of the membrane associated cytoskeleton to the intracellular cytoskeleton and the glycocalix to the extracellular matrix, the elastic properties of tissue may be controlled over a large range. The plasma membrane is extremely soft with respect to bending and shearing but practically incompressible with respect to lateral stretching. This unique combination of elastic properties allows cells such as erythrocytes to travel for several 100 km through our body without loss of material.

The most intriguing aspect is, however, that the lateral incompressibility (which prevents the loss of ions) is solely while the high flexibility is largely determined by the lipid/protein bilayer.

From the point of view of membrane physics most fascinating, however, is the vesicle-mediated material transport between the various intracellular compartments and between these and the plasma membrane illustrated in Fig. 2. It involves a manifold of shape changes and shape instabilities, including the vesicle budding–fission–fusion chain of events.

One purpose of my talk is to show that many of these complex processes may be understood in terms of the bending elasticity concept of bilayer shells. In the first part I will briefly summarize the essential role of lipid bilayer elasticity for the self organization of biomembranes and the formation of specialized domains such as coated pits and buds. The second part deals with the minimum-bending-energy concept of shape transitions of pure one component, lipid vesicles and the essential role of the constraints imposed by the closure of the shells and their stratified composition. In the third part I will introduce the enormous richness of shape transitions of membranes composed of lipid/protein - alloys which is determined by the coupling between curvature and phase separation and chemically induced bending

*Corresponding author. Fax: (49) (89) 3209 2469.

The previous Datta Lectures were given by: F. Melchers (1st, 1986); N. Sharon (2nd, FEBS Letters (1987) 217, 145–157); B.G. Malmström (3rd, FEBS Letters (1989) 250, 9–21); J.C. Skou (4th, FEBS Letters (1990) 268, 314–324); B.A. Lynch and D.E. Koshland, Jr. (5th, FEBS Letters (1992) 307, 3–9); A.R. Fersht (6th, FEBS Letters (1993) 325, 5–16).

Abbreviations: PC, phosphatidyloholine; DMPC, dimyristoylphosphatidylcholine; DMPG, dimyristoylphosphatidylglycerol; RICM, reflection interference contrast microscopy.

SSDI 0014-5793(94)00484-D

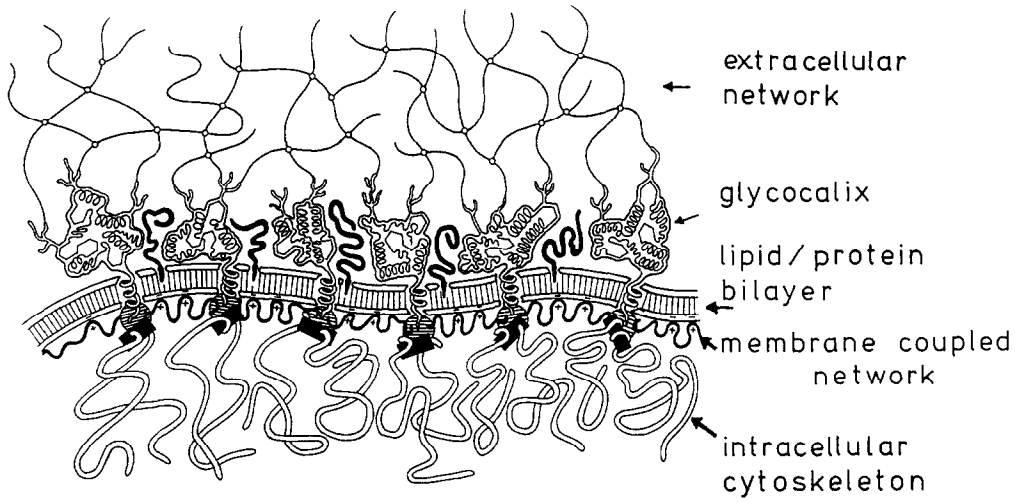

Fig. 1. Cartoon of the coarse structure of the cell plasma membrane and associated networks of the intracellular cytoskeleton and the extracellular matrix. The caricature emphasizes the three-layered structure of the membrane consisting of three types of materials. The lipid/protein-bilayer which may be considered as two-dimensional smectic liquid crystal. The membrane associated cytoskeleton which forms a two-dimensional macromolecular network and the glycocalix which is essentially a two-dimensional macromolecular layer. The membrane is a composite material since a structural change in one layer is supposed to induce a corresponding change in the other two.

moments. The last part deals with thermally excited undulations of membranes and their possible biological functions.

2. Principles of vesicle self assembly and stabilization

Nature was extremely clever by choosing two-chain lipids as basic building units of membranes for the following reasons:

1. They associate in water at extremely low concentrations ($< 10^{-12}$ M). This is a consequence of the very large hydrophobic effect and the well known exponential dependence of the critical concentration of association c^* on the work (= chemical potential $\Delta\mu$) required to transfer a lipid molecule from the bilayer (or a micelle) into the aqueous phase [2]

$$c^* = c_o \exp\{-\Delta\mu/k_B T\}$$

$\Delta\mu$ is roughly proportional to the total area of the surface of the hydrocarbon chain and thus to the chain length n_{CH_2}. It can be estimated from the rule of thumb $\Delta\mu = 2(11-3n_{CH_2})$ [1,2]. The chemical potential differences for two-chain lipids are very high: typically $\Delta\mu = -75$ kJ/M (or $\approx 30\ k_B T$) for a chain of 16 CH_2-groups. It is due to the exponential law, that the critical micelle concentration is so much higher for lyso-lipids ($c^* \approx 2 \cdot 10^{-5}$ M for Lyso-DMPC) than for normal lipids ($c^* \approx 2 \cdot 10^{12}$ M for DPPC).

2. A consequence of the strong hydrophobic effect is a very high (and negative) internal lateral tension within bilayers of the order of 30 mN/m. It is for that reason that bilayers exhibit strong self-healing effects.

3. Bending energy concept of vesicle closure. In excess water, most lipids spontaneously form closed shells which exhibit an astonishing high stability as illustrated in Fig. 3. Vesicle formation may be understood as payoff between the energy required to bend the bilayer and the energy gained by avoiding the exposure of the hydrophobic interior of the bilayer to water [3]. Let us have a closer look at the process which allows simultaneously to introduce the bending energy concept. In order to bend the bilayer a positive tension (σ_+) has to be applied at one monolayer and a negative (σ_-) at the other which results in a bending moment $M = d_m(\sigma_+ - \sigma_-)$ (where d_m is the membrane thickness). Any curved surface may be characterized by the average curvature $(1/R_1 + 1/R_2)$ where R_1 and R_2 are the principal radii of curvature (measured along two perpendicular directions). Hook's law states that

$$M = K_c(1/R_1 + 1/R_2)$$

where K_c is the bending elastic modulus (which is measured in units of energy since the dimension of σ is mN/m). The total energy associated with bending is given by

$$G_{bend} = \frac{1}{2} K_c \int (1/R_1 + 1/R_2)^2 \, d0 \qquad (1)$$

where the integral has to be performed over the whole bilayer surface. The most remarkable consequence of Eq. (2) is that the bending energy of a sphere does not depend on its size (that is it is scale invariant).

In order to assess the interfacial energy at the edge of an open bilayer, consider a partially closed shell with an

opening of radius ρ. The total energy may be expressed as:

$$G_{pore} = 2\pi\gamma d_m \rho$$

where γ is the line tension along the rim of the pore (measured in N/m). Minimizing the total energy yields for the vesicle radius

$$R_o = 8K_c/\gamma \cdot d_m \quad (2)$$

The line energy per unit length γd_m of the opening may be estimated from the chemical potential of the hydrophobic effect by assuming that half of the surface of the lipid chains at the edge of the bilayer is exposed to water. For DMPC this would correspond to $\Delta\mu = 5 \times 10^{-20}$ J per molecule or $\gamma d_m = 5 \times 10^{-11}$ N. The edge energy of a flat piece of membrane of 10 μm diameter would thus be of the order of $3 \times 10^5\ k_B T$. The bending energy of the vesicles (of all sizes) is about $100 k_B T$. Hence the driving force for vesicle closure is very high.

The key point is that both the pore energy and the bending energy can be drastically reduced by suitable solutes.

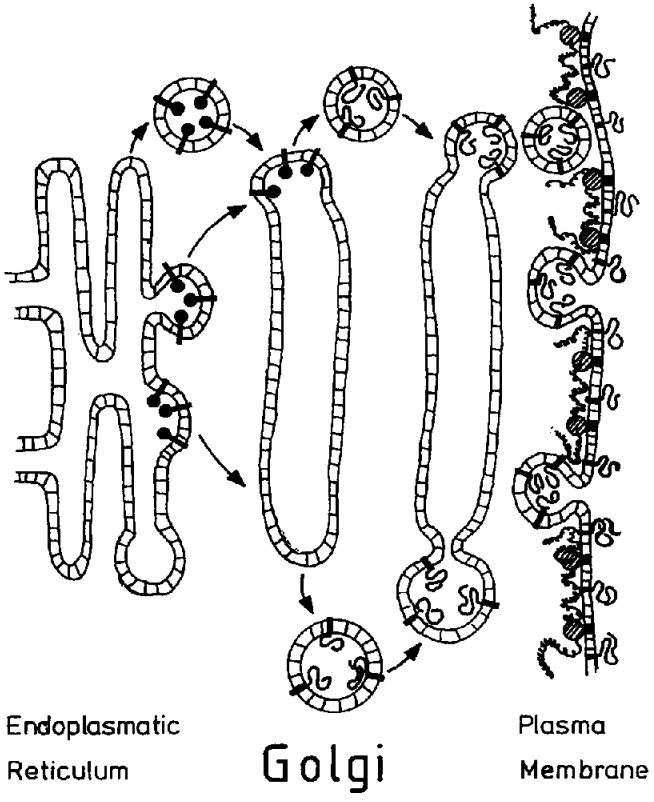

Fig. 2. Illustration of (one way of) intracellular transport from Endoplasmatic Reticulum to the plasma membrane mediated by vesicles and demonstrating the necessity of vesicle budding–fission–fusion chain of events. Note that fusion with the plasma membrane requires the transient decoupling of the cytoskeleton from the bilayer.

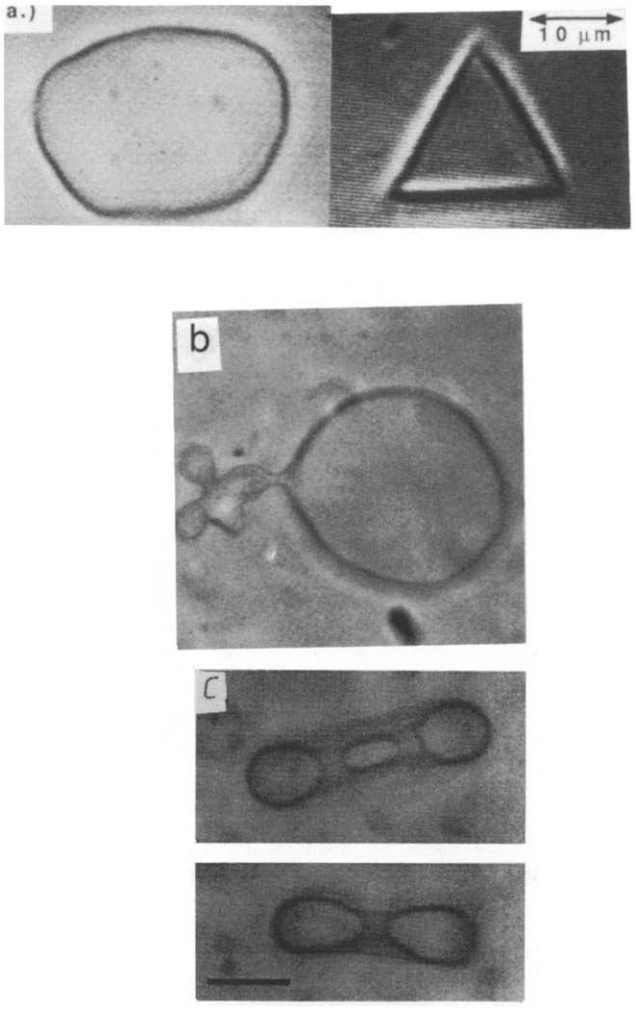

Fig. 3. Demonstration of stability of single bilayer vesicles. (a) Shape change of giant DMPC vesicle in 500 mM Na Cl buffer at fluid to gel transition. Note the astonishing stability of the vesicle composed of a crystalline shell. Vesicle diameter 10 μm. (b) Spontaneous budding of DMPC vesicle leading to tube-like (sometimes branched) protrusions. Vesicle diameter 20 μm. (c) Torus shaped vesicle of diacetylene-PC according to Bensimon et al. [17] Bar = 10 μm.

1. The pore energy may be reduced by surfactants which can form a hydrophilic cap at the rim of the pore. Large pores can thus be stabilized by digitonin or filipin in the presence of cholesterol. Even discs of bilayers may be formed at high concentrations of cholate [4].

2. The bending energy may be drastically reduced by introduction of a spontaneous curvature C_o which reduces the bending energy (per unit area) for the sphere to

$$g_{el} = \frac{1}{2} K_c (2/R - 2C_o)^2 \quad (3)$$

A spontaneous curvature can be generated by any gradient of the lateral pressure $d\pi r/dz$ in the direction (z) of the bilayer normal which creates a bending moment (cf. Fig. 4)

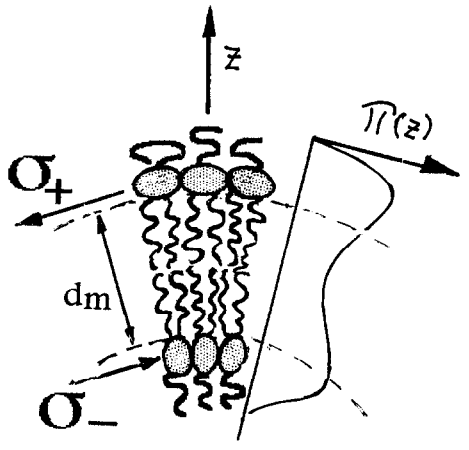

Fig. 4. Illustration of generation of (one-dimensional) intrinsic bending moment, M, by gradient of lateral pressure $\pi(z)$ across the bilayer. The bending moment may also be represented by a couple of opposite tensions (measured in mN/m).

$$M_o = \int_{-d_m/2}^{+d_m/2} z\pi(z)\,dz \quad (4)$$

resulting in a spontaneous curvature $C_o = M_o/K_c$.

There are many ways to create intrinsic bending moments, in particular by the adsorption of proteins (as in coated pits) or by changing the surface charge density (e.g. by the binding of Ca^{2+}). The spontaneous curvature concept is also extremely helpful for the understanding of the micelle–bilayer transition [5].

3. Elasticity of bilayer–cytoskeleton composite membranes

3.1. Modes of deformation

Any deformation of cell membranes can be described in terms of a superposition of the three modes of deformation well-known from the classical theory of shells

1. pure bending (introduced above)
2. pure shearing and
3. isotropic compression.

The resistance of bilayers towards isotropic tension (compression or dilatation) is characterized by the elastic energy (per unit area)

$$g_{comp} = \frac{1}{2}\kappa\left(\frac{\Delta A}{A}\right)^2 \quad (5)$$

where $\Delta A/A$ is the relative change in bilayer area and κ is the lateral compressibility modulus measured in J/m^2. The tension required to maintain the area change is $\sigma = \kappa\Delta A/A$.

The compressibility modulus and the bending modulus are proportional to each other

$$\kappa = K_c/d_m^2$$

Pure shearing is best visualized by considering a square piece of bilayer which is stretched in one direction by a tension σ_+ to a length $L = L_o + \delta L$ and compressed to $L = L_o - \delta L$ in a perpendicular direction by a tension (of the same size). Clearly the area remains constant for this type of deformation. It is customary to express the strain in terms of the elongation ratio $\lambda = (L_o + \delta L)/L_o$ and the energy is then given by [13]

$$g_{shear} = \frac{1}{2}\mu(\lambda^2 + \lambda^{-2} - 2) \quad (6)$$

where μ is the shear elastic constant.

Some data: Many sophisticated techniques have been developed for high precision measurements of the elastic constants of vesicles and cell membranes such as the micropipette technique [13], the electric field deformation technique [14] and the flicker spectroscopy [16]. Some data are shown in Table 1.

These studies have revealed outstanding elastic properties of biological membranes. This is best demonstrated by comparing the elastic constants of erythrocytes with those of a shell made of a synthetic polymer exhibiting the same size and topology (cf. data in Table 1). The most remarkable finding is that the cell membrane is extremely soft with respect to bending and shearing but is laterally incompressible. This combination of elastic constant allows the cell to squeeze through very narrow channels without loss of ions [6,14].

Two other remarkable findings are:

1. Despite of the high cholesterol content and the bilayer–cytoskeleton coupling, the bending stiffness of the erythrocyte membrane is equal to about that of DMPC-bilayers.
2. The cell exhibits a shear free deformation regime and stiffens with increasing deformation.

3.2. Modulation of bilayer elasticity by solutes

The membrane elasticity may be manipulated in various ways (cf. Table 1).

Incorporation of small amounts of amphiphiles may reduce the bending stiffness dramatically. Thus, addition of 1% of cholate reduces the K_c-value of DMPC by a factor of 10. Even more dramatic effect arise if small bipolar lipids are incorporated reducing K_c to the order of thermal energy which results in extremely drastic fluctuations [16]. Thus the low bending stiffness of the erythrocyte membrane could be due to solutes.

The bilayer elasticity is determined by the lateral packing density. Therefore the well-known condensing effect

of cholesterol leads to a strong increase of the bending and compression modulus.

3.3. Modulation of erythrocyte bending stiffness (cf. Fig. 5)

The softness of the erythrocyte membrane is still an enigma. An important observation is that the effective stiffness is remarkably increased:

1. By cross-linking of the spectrin/actin network by diamid [14].

2. By coupling of the network to glycophorin via band IV.1 (which is mediated by the binding of antibodies or wheat germ agglutinin to glycophorin).

3. By ATP-depletion (which randomizes also the transmembrane lipid asymmetry [9]).

These observations suggest that the membrane softness is maintained by continuous phosphorylation of the cytoskeletal proteins. Thus, phosphoylation reduces the bending of ankyrin to band III. and of band IV.1 to glycophorin by a factor of about 5. A partial decoupling of the network from the bilayer (mediated by phosphorylation) appears to be essential for the maintainance of the high degree of softness (cf. Fig. 5).

4. Lateral stucture formation in membranes

Over the last twenty years it has become more and more evident that biological membranes, in particular the plasma membranes, exhibit non-random lateral organization despite of the fact that the lipid bilayer moiety is in the fluid state. Indeed, direct evidence for a non-random bilayer organization has been provided by local lateral diffusion measurements and more recently by optical near field microscopy [15].

Several mechanisms of lateral structure formation are conceivable:

1. Coupling of membrane proteins and possibly lipids (Fig. 5) to the cytoskeleton.

2. Formation of local buds which may be induced by a protein adsorption (as in the case of coated pits) or other local bending moments (cf. Fig. 4).

3. Local phase separation within the two-dimensional lipid/protein multicomponent system.

Table 1
Comparison of two-dimensional elastic moduli of biological and technical materials

Material	Shear modulus, μ (erg/cm^2)	Compressibility modulus, χ (erg/cm^2)	Bending modulus, K_c (erg)
Brass	1×10^5	10^5	10^{-8}
Polyethylene	5×10^3	5×10^3	5×10^{-10}
Erythrocyte	6×10^{-3}	–	7×10^{-13}
DMPC bilayer Lα-phase	0	145	1.2×10^{-12}
DMPC with 30% cholesterol	0	647	4×10^{-12}
DMPC with 5% cholate	0	–	1×10^{-13}

In the following I will briefly discuss the last two mechanisms and start with the last one. A large amount of work on lipid mixtures has been accumulated (cf. [6,18]). Concerning the question of lateral structure formation in biomembranes the following findings are essential.

1. Phospholipid mixtures exhibit in general phase diagrams of the form shown in Fig. 6. Phase separation arises in general only if one of the components is in the gel state. Indeed some of the natural lipids of mammalian cells exhibit very high transition temperatures. Thus, brain sphingomyelin (SPM) exhibits a very broad regime of fluid–solid coexistence from 30 to 60°C [7] making lateral phase separation in nerve membranes at physiological temperatures quite probable.

2. In the presence of Ca^{2+} the phase transition temperature of charged lipids is strongly shifted to higher temperatures (by about 50°C). Ca^{2+} influx in cells can thus easily generate local domain formation in the inner leaflet of plasma membranes. Since the Ca^{2+}-induced domain formation exhibits a very strong hysteresis, even a transient increase of the intracellular Ca^{2+} level (e.g. in synapses) can result in metastable domain formation [6,19].

3. There is only one well-documented example of fluid–fluid immiscibility, namely the PC–cholesterol mixture (cf. [18]). This mixture exhibits a miscibility gap between about 10 and 30 mol% cholesterol and the critical point lies about 30°C above the gel-fluid transition of the PC. Physiologically even more important is, however, that cholesterol-rich domains occur at concentrations of about 40mol% as has been conclusively shown by small angle neutron scattering studies (cf. [6]). Some evidence for the segregation of cholesterol in erythrocytes is provided by the observation that erythrocytes membranes exhibit a fraction of rapidly exchangeable cholesterol while a large fraction is only slowly exchangeable. The latter fraction could be organized in clusters. We will show below that the local clustering of cholesterol may play an important role for the vesicle fission after osmotic deflation of intracellular compartments.

4. A highly interesting situation arises for lipid mixtures exhibiting a miscibility gap in the solid state with a critical point lying within or slightly below the fluid solid coexistence. For the particular case of the DMPC/DSPC mixtures it has been shown by small angle neutron scattering that the mixture exhibits lateral heterogeneity even well above the liquidus line which is due to critical demixing [20]. Segregated domains of the high melting component exhibiting average diameters of about 300 Å form roughly 10°C above the liquidus line. Very detailed Monte Carlo simulations have shown that this is in general expected for mixtures of lipids differing in chain length by more than 4 C-atoms [18]. It is therefore well-probable that critical demixing is quite common in biomembranes. The most interesting aspect is, however,

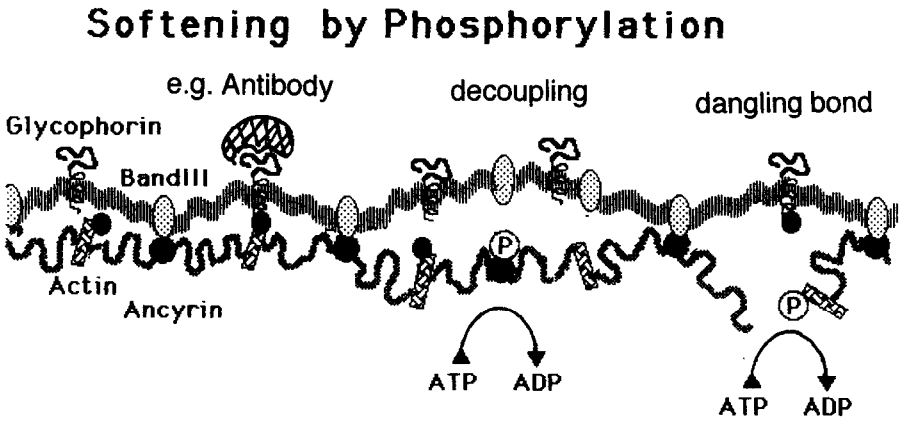

Fig. 5. Illustration of fine-tuning of coupling of lipid/protein bilayer to spectrin-actin network of erythrocytes by phosphorylation of coupling proteins ankyrin and band 4.1. The strong weakening of the coupling strength after phosphorylation may result in the decoupling of the cytoskeleton from the bilayer or the formation of dangling bonds (right) within the cytoskeleton which increases the membrane flexibility. Binding of ligands (e.g. antibodies) to glycophorin can result in a strengthening of the coupling and thus in an increase in stiffness.

that the transient domains would be stabilized by proteins, provided selective lipid/protein interaction mechanisms exist (cf. [6]). This point is discussed below.

5. Mechanisms of selective lipid protein interaction

The local structure formation by clustering is closely related to the existence of mechanisms of selective lipid/protein interaction. Two mechanisms have been established hitherto: an electrostatic and a steric elastic mechanism (which are illustrated in Fig. 7). The former mechanism arises if the hydrophobic thicknesses of the lipid bilayer d_m and of the protein d_p are not matched. Thus, if $d_m < d_p$ the hydrocarbon chains of the lipids adjacent to the protein are stretched in order to avoid exposure of the hydrophobic parts of the protein to water. An interesting question is how far the perturbation of the lipid matrix extends. Many theoretical studies (cf. [18] for references) postulate that the perturbation decays exponentially with the distance from the surface of the protein (of radius r_p)

$$(d_m - d_p) = (d_m - d_p)_o \exp\{-(r - R_p)/\zeta\} \quad (7)$$

where ζ is the correlation length which is about $\zeta = 30$ Å (corresponding only to 2 to 3 lipid distances). Nevertheless, the energy associated with the deformed lipid halo is substantial and depends on the bilayer compressibility modulus. For a mismatch of $(d_m - d_p) \sim 5$ Å, the total elastic energy is about 100 $k_B T$. This has far-reaching consequences in mixtures of lipids of different chain length since the protein will surround itself by a halo of length-adapted lipid as illustrated in Fig. 7.

The electrostatic mechanism of lipid/protein selectivity has been established in many model membrane studies. In particular, many of the actin binding proteins mediating the interaction of actin with the membranes such as talin and hisactophilin or α-actinin bind to membranes in the presence of charged lipids (cf. reference [21]). A direct interaction of talin with the lipid bilayer is also suggested by the finding that a large fraction of this protein is bound to the lipid/protein bilayer and can only be removed by surfactants (e.g. Triton).

Membrane bound receptors may simultaneously exhibit the steric elastic and the electrostatic mechanism of selective lipid protein interaction. A well studied example is the transferrin receptor [22]. First it was shown that a substantial amount of this receptor can only be incorporated in bilayers if the hydrocarbon chains are long enough (> 16 C-atoms) and in the presence of acid lipids. As demonstraded by calorimetry and Fourier-Transform-Infrared-Spectroscopy (cf. Fig. 8b), the protein interacts preferentially with charged lipids. This is attributed to to the binding of a sequence of acidic amino acids of the cytoplasmatic domain to the charged lipids (cf. Fig. 8c).

6. Bending energy concept of vesicles and cell shape changes

Giant vesicles of a single lipid component (such as DMPC) show a very rich scenario of shapes and shape transitions many of which are familiar from biology. Fig. 9 exhibits a series of characteristic and typical examples of transitions generated by variation of the excess area of the bilayer by heating: Fig. 9a shows an initially quasispherical vesicle which first changes into a discocyte which is stable over a rather large range of area-to-volume ratios before it undergoes a transition into a stomatocyte. The transition is completely reversible. As shown in Fig. 9b, a completely different behaviour is observed when the vesicle was kept under high osmotic stress be-

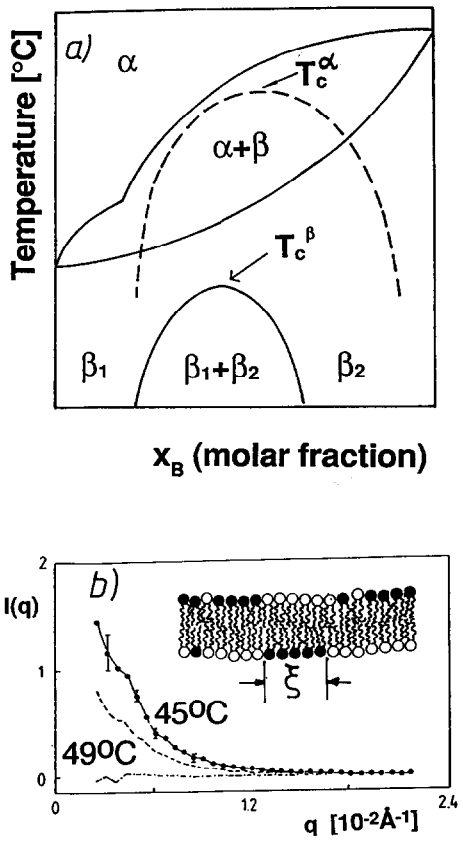

Fig. 6. (a) Hypothetical phase diagram of binary mixture of lipids. It exhibits in general peritectic behaviour of the fluid-solid coexistence ($\alpha + \beta$) if a solid-solid miscibility gap ($\beta_1 + \beta_2$) penetrates into the coexistence region. For the same type of lipid, the critical point is shifted to higher temperatures with increasing differences in chain lengths. Most remarkably, critical demixing of the lipids is observed above the liquidus line [20]. (b) Demonstration of critical demixing in mixture of DMPC and DSPC above the liquidus line. The plots of the scattering intensity as a function of scattering angle show that the average cluster size increases dramatically if the critical point is approached, The cluster is $\xi < 500$ Å at 45°C and 300 Å at 49°C. The critical temperature is $T_c < 40$°C.

fore heating. Within a very narrow temperature interval (corresponding to an area increase of 7%) buds and tethers shoot out which eventually merge. Fig. 9c shows the case of a transition from a quasispherical shape to a stomatocyte caused by osmotic deflation.

In the following it will be shown that shape changes of vesicles (but also of cell membranes) can be explained in terms of the minimum bending energy hypothesis which predicts that the global shape of a soft shell is determined by the minimum of the total bending energy subjected to the constraints [10,11]

1. of constant average area (A) which holds if the exchange of lipids with the environment is blocked

2. of constant area difference

$$\Delta A = A_o - A_i \quad (8)$$

between the outer (o) and inner (i) leaflet (which holds for blocked lipid exchange between the monolayers).

Two modes have been proposed: the spontaneous curvature model presented by Eq. (2) and the bilayer coupling model.

The bilayer coupling model enables a simple physical interpretation of the shape changes by considering the area difference ΔA. For a sphere of radius R_o it is $\Delta A = 8\pi R_o \cdot d_m$. In order to generate a stomatocyte, the inner monolayer has to be expanded with respect to the outer. To form for instance two interconnected spheres each of radius $R_o/\sqrt{2}$ the area difference (at constant volume) has to be $\Delta A_o = 8\sqrt{2}\,\pi \cdot R_o \cdot d_m$. Budding to the outside thus requires expansion of the outer monolayer with respect to the inner.

In the framework of this model, the possible shapes of two-layered shells may be expressed in terms of only two parameters

1. The degree of deflation, expressed in terms of the ratio v of the actual volume and the volume of a spherical vesicle of the same membrane area $<A>$.

2. The area difference Δa normalized with respect to the value $\Delta A_o = 8\,\pi \cdot R_o \cdot d_m$ for the sphere.

The situation may be presented in terms of the phase diagram shown in Fig. 10 in which each shape is represented by a range of values (v, Δa). The major merit of such a phase diagram is that the physical origin of a shape change may be reconstructed from the observed pathway through the phase diagram. Thus it has been shown that the shape changes of Fig. 9a and b are a consequence of different coefficients of thermal expansivity at the outer and inner monolayer. In particular, it is clear that a given shape may be generated either by

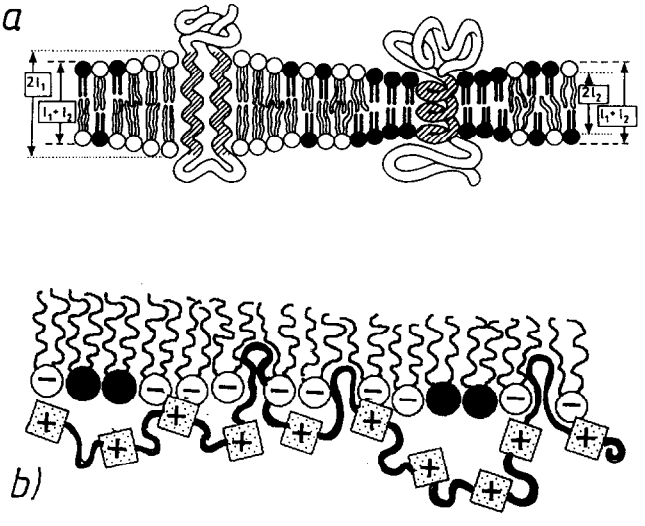

Fig. 7. On mechanisms of selective lipid–protein interaction. (a) Selective interaction due to mismatch of the thicknesses of the hydrophobic domains of the proteins and the lipid bilayer moiety. (b) Electrostatic selectivity illustrating binding of filamentous protein (e.g. spectrin) to bilayers. Neutron surface scattering studies suggest that the flexible hinges between the condensed domains penetrate into the bilayer.

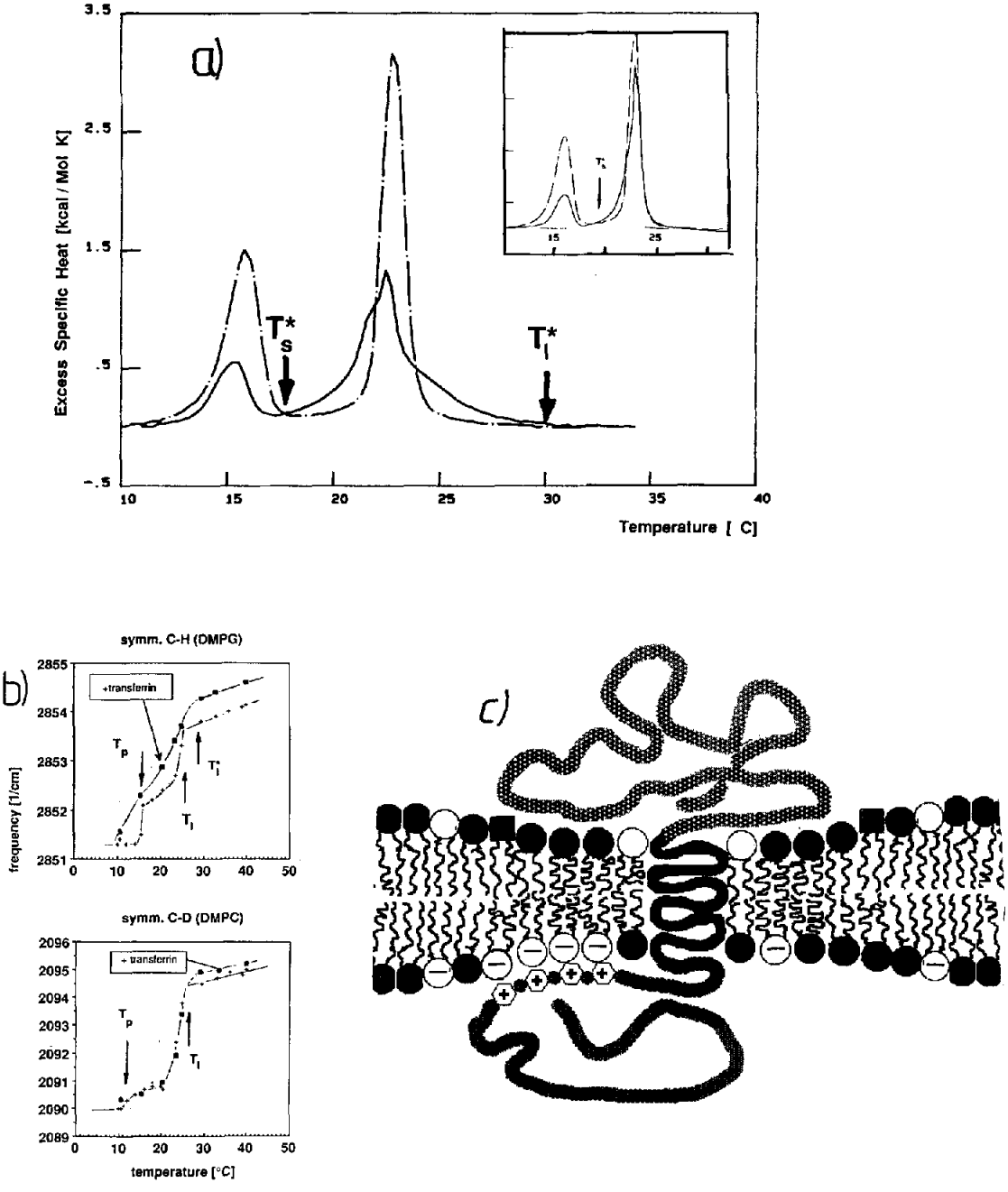

Fig. 8. (a) Calorimetic scanning curve of a 1:1 DMPC/DMPG mixture in absence (·····) and presence (—) of $x_p = 4 \cdot 10^{-4}$ transferrin receptor. The simultaneous shift of the upper transition (the liquidus line T_l) to higher and of the lower transition (the solidus line T_s) to lower temperatures is attributed to electrostatic interaction and to the elastic distortion of the hydrophobic domain, respectively. Inset shows the region of the main transition after removal of the head groups of the receptor by protease resulting in a suppression of the shift of T_l. (b) Demonstration of selective interaction of receptor with charged DMPG by Fourier Transform Infrared Spectroscopy. Note that only the phase transition of DMPG is affected by the protein (cf. Kurrle et al. [22]). (c) Model of combined elastic and electrostatic interaction.

changing the degree of deflation v or by changing Δa. Another important prediction is that the shape changes depend critically on the pre-history of the vesicle that is whether one starts from a flaccid or from an osmotically stressed vesicle [24]. This difference is clearly demonstrated in Fig. 9a and b.

7. Shape changes of mixed membranes, or coupling between curvature and phase separation

The scenario of shape changes becomes much richer for membranes composed of mixtures. The situation becomes very complex since the shapes of minimum bend-

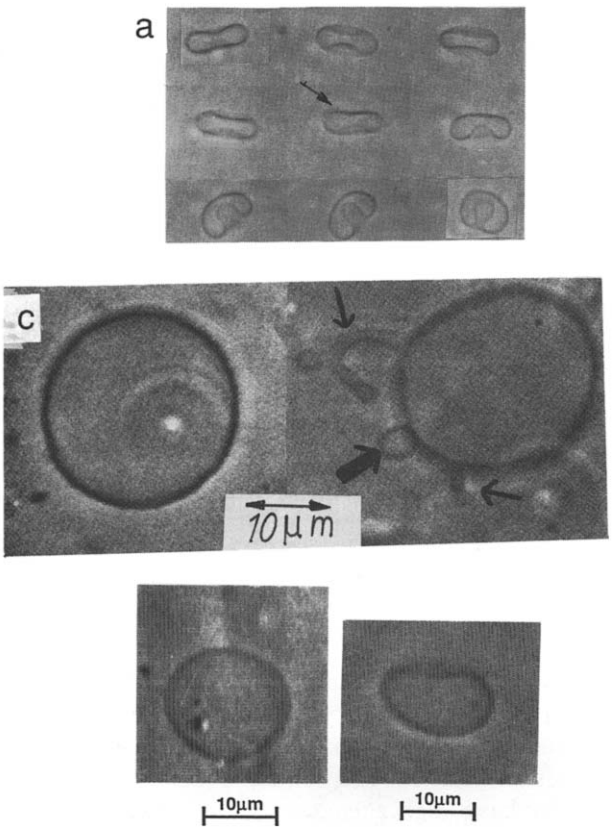

Fig. 9. Shape changes of pure lipid (DMPC) bilayer caused by increasing the excess area of the membrane by heating. (a) Discocyte-to-somatocyte transition of initially quasispherical vesicle. (b) Blebbing transition of DMPC vesicle in pure water by increase of the area by only about 7% (according to Käs and Sackmann [24]). (c) Example of spontaneous curvature-induced shape change of DMPC originally prepared in 200 mosm inositol. Left: outside medium contains 200 mM inositol. Right: shape observed after replacing outside medium by 178 mM inositol and 11 mM NaCl.

ing energy are determined by three additional factors such as

1. the transmembrane asymmetry;
2. the different spontaneous curvatures of regions of different composition;
3. the interfacial energy between regions of different composition.

Let us consider first some experimental finding:

In Fig. 11 we show that lateral phase separation may lead to a stable domain structure instead of a complete separation of the components as one would expect for ordinary mixtures. In the case of the DMPC-DMPE mixture in the fluid–solid coexistence (Fig. 11a), the DMPE-rich phase is solid and therefore exhibits completely flat domains while the DMPC-rich domains are fluid and exhibit the same average curvature as the vesicle.

Fig. 11b shows the situation of lateral lipid segregation caused by the adsorption of a charged polypeptide (polylysine) to a vesicle containing charged lipids (phosphatidic acid). The polypeptide causes segregation of the charged lipid which forms, however, only small domains. Again it is important to realize that the two phases exhibit different local curvatures. Below we will argue that the stabilization of the domain structure is a consequence of an elastic interfacial energy which prevents the growth of domains.

Domain formation is essential for the stabilization of heterogeneously organized membranes since complete segregation would result in decay of the vesicles into frations of different composition (cf. reference [6])

Fig. 12 shows an example of the coupling between curvature and phase separation in a fluid vesicle. An amphiphilic macrolipid is grafted to the outer monolayer of DMPC-vesicles by hydrophobic chains. The hydrophilic polymer chain undergoes a transition from an expanded to a collapsed state above a lower critical point at $T_c \sim 32°C$. If the polymer is in the expanded state, the vesicles tend to exhibit nonaxially symmetric shapes (such as the triangular shape of Fig. 12a). Heating through the expanded-collapsed transition leads to budding of the single-walled vesicles while the vesicles with multilamellar shells form only soft protrusions.

The formation of vesicles of non-axially symmetric shape (which is rarely observed for one-component vesicles) is a consequence of the coupling between phase separation and curvature. The expanded macrolipid prefers areas of high convex curvature and thus tends to accumulate in the protrusions. The entropy of mixing and the repulsion between the head groups, however, counteracts this lateral phase separation. Therefore only a slight distortion of the vesicle with a small non-random lateral distribution of the macrolipid is expected.

This type of shape transition can be described in a very general way by combining the Cahn–Hilliard–Langer theory of spinodal decomposition with the minimum bending energy concept. This mathematically very complex problem is treated elsewhere [6,25,26]. The complete budding caused by the collapse of the polymer is a consequence of two effects:

1. the strong positive bending moment caused by contraction of the hydrophilic head groups and
2. the strong decrease of the entropy of mixing.

Fig. 12b shows that the curvature of the buds depends critically on the bending stiffness K_c of the vesicle shell. According to Eq. (3), the spontaneous curvature C_o (or ΔA_o) is inversely proportional to K_c. This explains why the complete budding is found for unilamellar vesicles while the polymer collapse generates only softly curved protrusions in multilamellar vesicles. The bending stiffness of a shell of n bilayer is nK_c. The most intriguing aspect of the experiment shown in Fig. 12 is that the polymer induced shape changes are reminiscent of coated pit or vesicle formation.

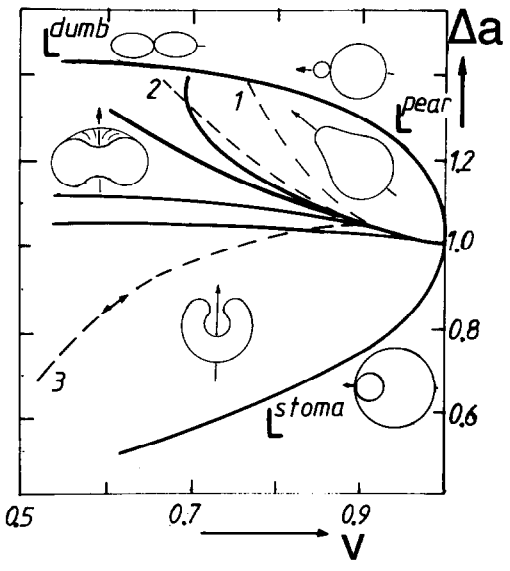

Fig. 10. Phase diagram of vesicle shapes as calculated by the bilayer coupling model. Δa and v are reduced values of the area difference and the volume (cf. Berndl et al. [34]). Note that $\Delta a > 0$ corresponds to a positive and $\Delta a < 0$ to a negative spontaneous curvature. For a sphere (which is not under high osmotic tension) $\Delta a = 1$ and $v = 1$. The dashed curves 1, 2, 3 denote observed paths of shape changes [24].

8. Domain stabilization versus vesicle fission

The fission of budded vesicles which is seldomly observed for one-component fluid vesicles is quite common for mixed vesicles. One example is shown in Fig. 13a another, of more direct biological relevance is shown in Fig. 13b. These findings appear to contradict the formation of the stable domain structure in vesicles undergoing phase separation. In order to understand this discrepancy, we have to consider the interfacial energy at the boundary between different phases more closely. As shown in Fig. 14, an elastic and a chemical contribution has to be considered which exert opposite effects on the vesicle stability. The former arises if the two phases exhibit different spontaneous curvatures. The local variation of the lipid orientation at the interfaces (called splay elastic deformation in liquid crystal physics) is associated with an elastic bending energy. It is easily seen that the interfacial energy increases with the radius p of the domains. A simple consideration yields $\gamma_{if}^{el} \propto \rho^2$ Thus, the total interfacial energy of a domain increases with its radius as $G_{if}^{el} \propto 2\pi\rho^3$. It is thus clear that the elastic interfacial energy impedes the growth of the domains.

The chemical contribution to the interfacial energy per unit length γ_{if}^{ch} is constant and is independent of the domain size. As shown by Lipowsky [27], the total interfacial energy G_{if}^{chem} could be drastically reduced by budding in such a way that the interface is located in the narrow neck interconnecting mother and daughter vesicles. This process is only possible in vesicles exhibiting excess membrane area. The size of the bud is determined by the condition that the bending energy associated with the bud formation is compensated by the gain in interfacial energy. A simple consideration (similar to that leading to Eq. (2)) yields for the radius of the bud

$$R_B = 8K_c/\gamma_{if}^{ch} \quad (9)$$

An example of this budding mechanism is shown in Fig. 13a. The natural brain sphingomyelin exhibits a very broad phase separation regime between 30 and 50°C (that is under physiological conditions). Heating of the vesicle generates excess membrane area and causes continuous melting of some of the lipids. The vesicle buds detach rapidly from the mother vesicle which remains essentially spherical. A closer inspection of the freeze fracture electron microscopy images shows that the composition of the buds is different from that of the mother vesicle.

The process shown in Fig. 13a could well play a role for lipid sorting in cells. As is well-known, sphingomyelin resides mainly in the plasma membrane and the lysosomes (or CURL-vesicles, [8]). Thus the question arises how this lipid is preferentially recycled to the plasma membrane after endocytosis and fusion with the cytoplasmic vesicles (endosomes). Provided that sphingomyelin has a higher tendency for budding and fission from the CURL-vesicles than the other lipids it would preferentially be transported back to the plasma membrane.

The fission of the vesicle can also be driven by local phase separation within the neck. This is strongly suggested by the finding that lecithin vesicles containing a high cholesterol content ($\geq$ 40 mol%) exhibit fission after budding caused by osmotic increase in membrane excess area. This biologically relevant fission process is shown in Fig. 13b. Vesicles containing smaller cholesterol concentrations do not show fission. This is attributed to the fact that above about 40mol%, cholesterol exhibits local phase separation as was shown previously by small angle neutron scattering studies [28]. The vesicle fission is thus attributed to the accumulation of cholesterol within the neck interconnecting the vesicles.

9. Membrane undulations and their possible role for membrane processes

An important consequence of the extreme softness of fluid lipid bilayers is the excitation of pronounced bending undulations (so-called flickering). These ondulations are excited by thermal fluctuations (and are thus equivalent to Brownian motion). They are strongly overdamped due to the friction caused by the coupling of the undulations to hydrodynamic flows in the aqueous phase.

In order to get a feeling for the undulation amplitudes

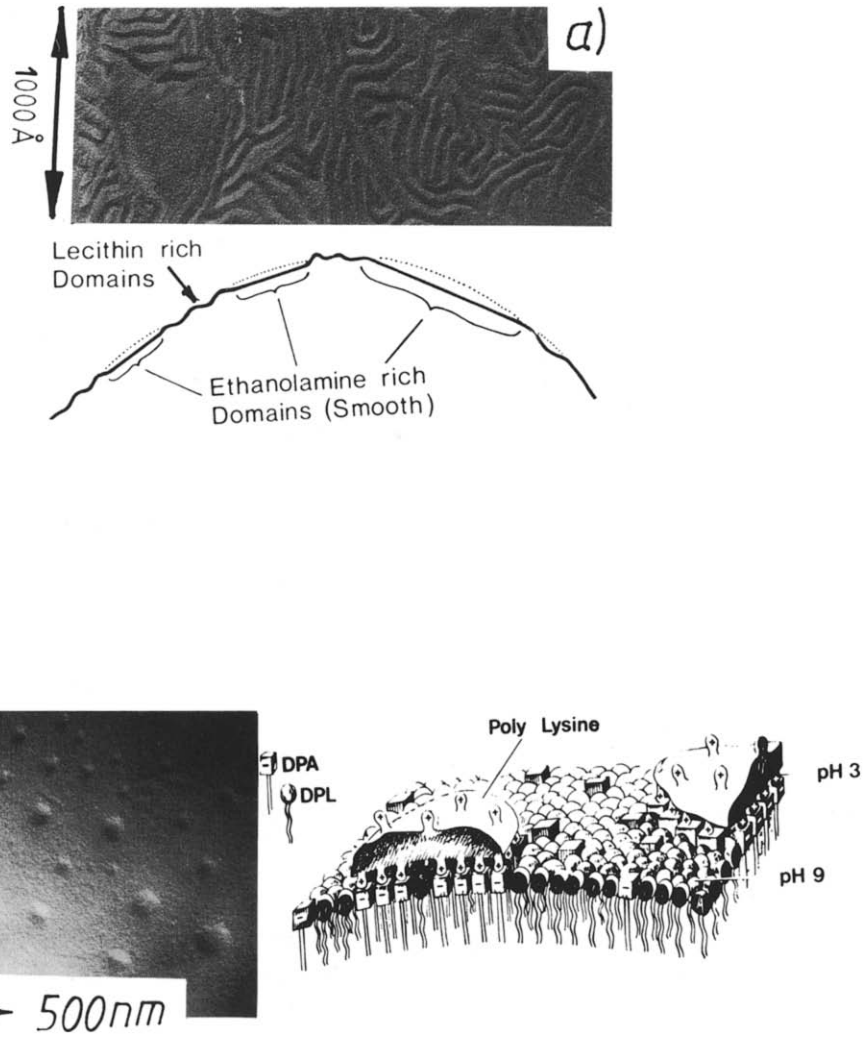

Fig. 11. (a) Stabilization of domain structure of vesicle composed of DMPC (50%) and DMPE (50%) in state of fluid-gel coexistence. Note that DMPE-rich domains are flat while the fluid DMPC-rich phase (wrinkled) exhibits the same curvature as the vesicle. (b) Domain formation in mixed vesicle containing a charged lipid component (phosphatidic acid) caused by the adsorption of randomly coiled polylysine.

we consider a piece of membrane of dimension $L \cdot L$. Any deflection of the membranes can then be described as a superposition of overdamped plane waves of wavelength $\Lambda = 2\pi/q$ where q is the wave vector.

$$U(\vec{r},t) = \sum_q U_q \cos(\vec{q}\,\vec{r}) \exp\{-\omega_q t\} \tag{10}$$

The bending energy is then simply given as a sum over all squared amplitudes of the individual modes of excitation

$$G_{\text{bend}} = \frac{1}{2} K_c \sum_q U_q^2 q^4 L^2 \tag{11}$$

Since each mode corresponds to a degree of freedom of the membrane, the equipartition theorem of the classical statistical mechanics may be applied which predicts that the average energy per mode is $1/2\ k_B T$. Therefore

$$\langle U_q^2 \rangle = k_B T / K_c q^4 L^2 \tag{12}$$

Since K_c is of the order of $10\ k_B T$, the amplitude of the longest wavelength mode of a bilayer of $L \approx 10\ \mu$m is $\langle |U_q|^2 \rangle \approx 3\ \mu$m, that is the undulation amplitudes are astonishingly high.

For closed vesicles the situation is more complex. The longest wavelength exitations are suppressed since the excess area of the bilayer is in general not sufficient for their full excitation. This constraint gives rise to a lateral tension [29] and the mean square amplitude is then changed into

$$\langle U_q^2 \rangle = \frac{k_B T / L^2}{K_c q^4 + \sigma q^2} \tag{13}$$

Clearly, the amplitudes are smaller for small q (or long wavelength).

The dynamic surface roughness associated with the

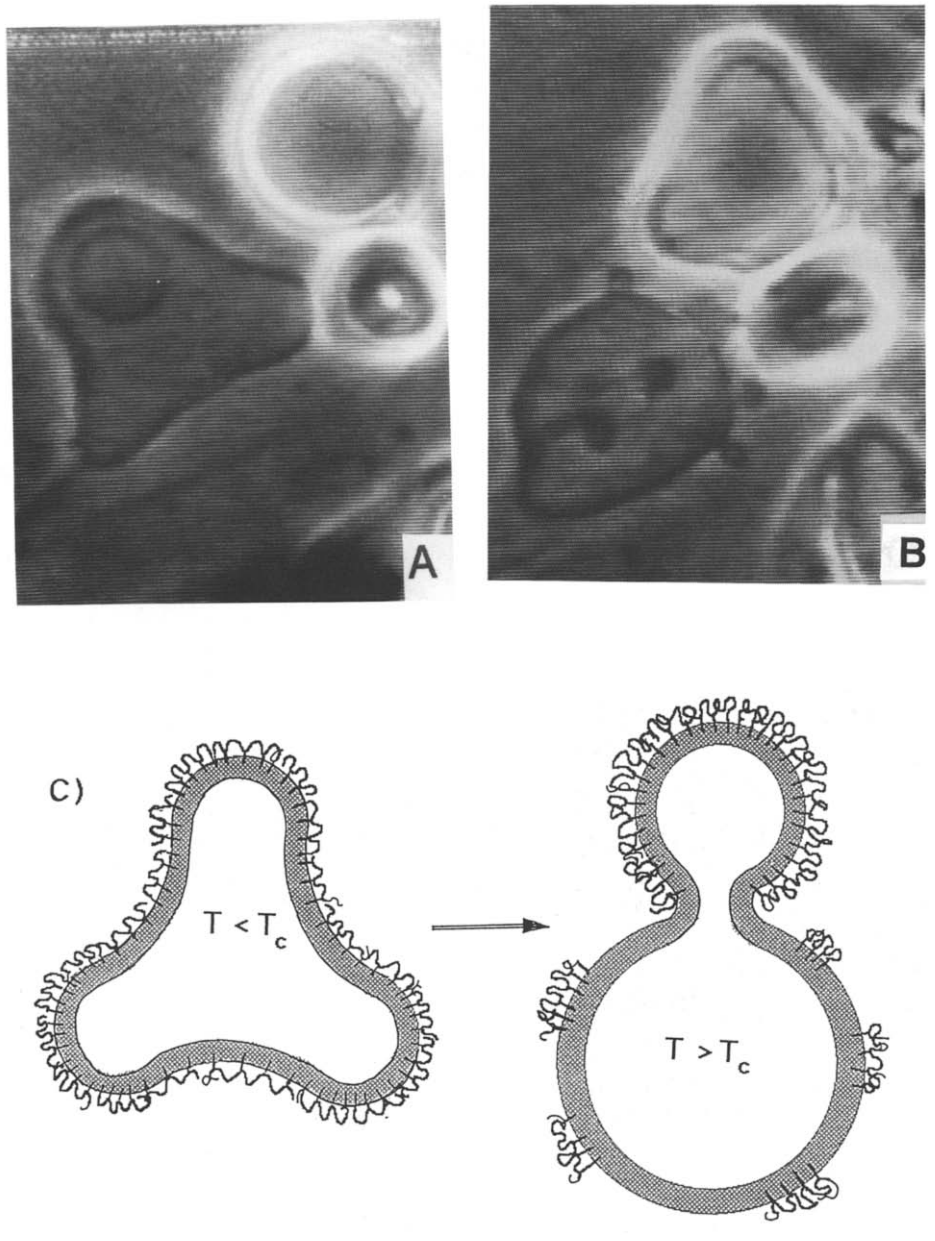

Fig. 12. Coupling between curvature and lateral segregation in vesicles of DMPC with macromolecular amphiphile which is anchored in the outer monolayer via hydrophobic chains and which exhibits an expanded to collapsed transition at $T > 32°C$. (a) (left side): Shape of vesicle with polymer in expanded state. Most remarkable is the non-axially symmetric (triangular) shape of the thin-walled vesicle (lower left corner). (b) (right side): Budding of vesicles after heating above the collapse point of polymer. Note that complete budding is only possible for thin-walled vesicle (lower left) while for multilamellar shells (upper right) only softly curved protrusions are possible. (c) Model of amphiphile structure and distribution.

undulations has many important consequences some of which will be discussed below.

A. Molecular exchange between membrane and cytoplasm: the coupling of the undulations to the aqueous environment leads to local hydrodynamic flows. These could help to facilitate the material exchange between the inner surface of plasma membranes and the cytoplasm, in particular in the erythrocytes.

B. Dynamic lateral tension: It is intuitively clear that a force is required to pull out the dynamic wrinkles. This amounts to a dynamic lateral tension as has been first shown by Helfrich [30]. This has an interesting consequence for in the erythrocyte plasma membrane. As indicated in Fig. 5 the bilayer exhibits a small excess area with respect to the spectrin–actin network and its undulations create a negative tension on the spectrin filaments (which can be considered as entropy springs [6]). One

may have the situation of two coupled springs one of which is stretched while the other is compressed (with respect to their resting states). Such a couple would indeed exhibit a nearly tension-free deformation regime. It is interesting to note that the tension associated with the undulations is equivalent to the entropy elasticity of macromolecules. Therefore lipid bilayers are two-dimensional analogues of semiflexible macromolecules such as actin [31].

C. Undulation force: The most spectacular consequence of the dynamic surface roughness is a dynamic repulsion force between flickering vesicles (or cells) and a solid surface (or between two vesicles or two cells). The undulation force predicted by Helfrich [30] can be directly observed and analysed by observation of the interaction of a vesicle with a glass substrate using reflection interference contrast microscopy (RICM) [32].

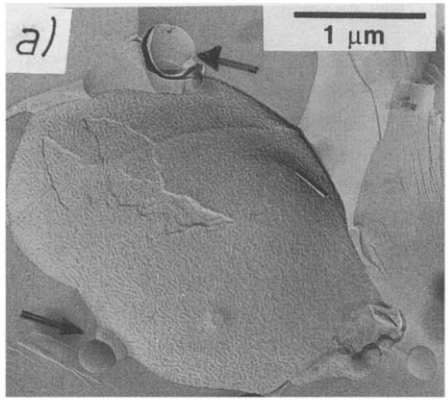

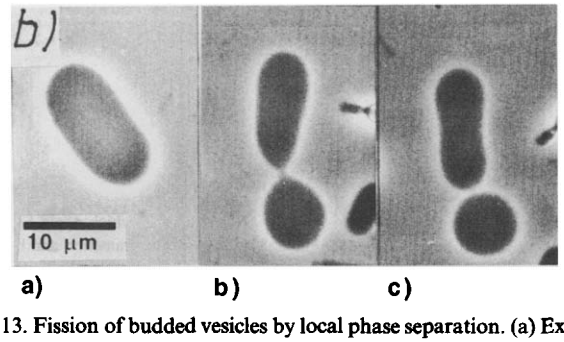

Fig. 13. Fission of budded vesicles by local phase separation. (a) Example of giant vesicle composed of brain sphingomyelin (freeze fracture electron micrograph). This mixture exhibits a broad fluid-gel coexistence between 30 and 50°C. Increasing the excess area by heating leads to budding but the buds detach immediately from the mother vesicle and swim away. (b) Osmotically driven fission of (60:40) DMPC/cholesterol mixture. The vesicle was deflated continuously by water outflux from the vesicle.

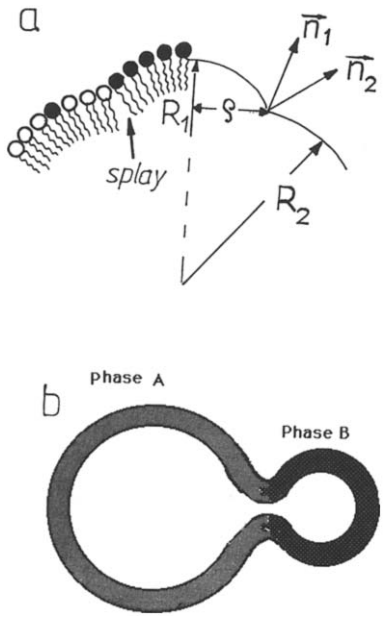

Fig. 14. Effect of elastic and chemical contribution to interfacial energy γ_{if} per unit length. (a) Splay deformation at interface between regions of different spontaneous curvature resulting in domain stabilization. Note that interfacial energy per unit length γ_{if} grows quadratically with the size, ρ, of the domain. (b) Reduction of chemical contribution to interfacial energy by budding resulting in a decrease of the length of the interface.

The origin of the undulation force becomes intuitively clear if one considers a flickering vesicle which approaches the surface to a distance h of the order of the undulation amplitude. Any further decreasing requires the gradual freezing-in of long wavelength modes or of more and more degrees of freedom. This corresponds to a reduction of the entropy associated with the thermal excitations and hence to an increase of the free energy. The situation is analoguous to the pressure excerted by an ideal gas if the available volume is reduced.

The situation depends upon whether the membrane is tension free or not. In the absence of tension, Helfrich derived a dynamic repulsive (disjoining) pressure of

$$P_{\text{und}} = \frac{3}{4}(k_B T)^2 / K_c\, h^3 \qquad (14a)$$

The most remarkable aspect is, that the distance dependence is the same as for the Van der Waals force. For a membrane under a tension σ an exponential law holds

$$P_{\text{und}} = (k_B T\, \sigma / 2h\, K_c) \exp\left\{ -\frac{2\pi\sigma}{3k_B T} h^2 \right\} \qquad (14b)$$

In fact, the latter situation is always expected for closed and adhering shells.

References

[1] Tanford, C. (1980) The Hydrophobic Effect, Wiley, New York.
[2] Cevc, G. and Marsh, D. (1978) Phospholipid Bilayers: Physical Principles and Models, Wiley, New York.
[3] Helfrich, W. (1974) Phys. Lett. 50A, 115–116.
[4] Fromherz, P., Roecker, C. and Rueppel, D. (1986) Farad. Disc. Chem. Soc. 81, 39–48.
[5] Gruner, A., Parsegian, A. and Rand, P. (1980) Farad. Disc. Chem. Soc. 81, 267–280.
[6] Sackmann, E. (1990) Can. J. Phys. 68, 1000–1012.
[7] Döbereiner, H.G., Käs, J., Noppl, D., Sprenger, I. and Sackmann, E. (1993) Biophys. J. 65, 1396.
[8] J. Darnell, J., Lodish, H. and Baltimore, D. (1990) Molecular Cell Biology, W.H. Freemann, San Francisco.
[9] Devaux, P.F. (1988) FEBS Lett. 234, 8–12.
[10] Seifert, U. and Lipowsky, R. (1990) Phys. Rev. A. 42, 4768–4771.
[11] Lipowsky, R. (1991) Nature 349, 475–481.
[12] Evans, E.A. (1974) Biophys. J. 14, 923–931.
[13] Evans, E.A. and Waugh, R. (1981) Biophys. J. 35, 637–652.
[14] Engelhardt, H. and Sackmann, E. (1988) Biophys. J. 54, 495–508.
[15] Hwang, J., Edidin, M., Betzig, E. and Chichestin, R.J. (1994) Biophys. J. 66, A277.
[16] Duwe, H. and Sackmann, E. (1990) Physica A. 163, 410–428.
[17] Mutz, M. and Bensimon, D. (1991) Phys. Rev. A. 43, 4525–4528.
[18] Bloom, M., Evans, E.A. and Mouritsen, O. (1991) Quart. Rev. Biophys. 24, 293–397.
[19] Knoll, W., Apell, H.J., Eibl, H. and Miller, A. (1986) Eur. Biophys. J. 13, 187–193.
[20] Knoll, W., Schmidt, G., Ibel, K. and Sackmann, E. (1985) Biochemistry 24, 5340–5246.
[21] Kaufmann, S., Käs, J. Goldmann, W.H., Sackmann, E. and Isenberg, G. (1992) FEBS Lett. 314, 203–205.
[22] Kurrle, A., Rieber, P. and Sackmann, E. (1990) Biochemistry 29, 8274–8282.
[23] Svetina, S. and Zeks, B. (1989) Biophys. J. 17, 101–111.
[24] Käs, J. and Sackmann, E. (1991) Biophys. J. 60, 825–844.
[25] Gebhardt, C. Gruler, H. and Sackmann, E. (1977) Z. Naturforsch. 32C, 581–596.
[26] Andelmann, D. Kavakatsu, T. and Kavasaki, K. (1992) Eur. Phys. Lett. 19. 57–62.
[27] Lipowsky, R. (1992) J. Phys. (France) 2, 1825–1828.
[28] Knoll, W., Schmidt, G., Ibel, K. and Sackmann, E. (1985) Biochemistry 24, 5240–5246.
[29] Millner, S. and Safran, S. (1987) Phys. Rev. A. 36, 4371–4379.
[30] Helfrich, W. (1978) Z. Naturforsch. 33a, 305–315.
[31] Sackmann, E. (1994) Macromol. Chem. Phys. 195, 7–28.
[32] Rädler, J. and Sackmann, E. (1993) J. Phys. (France) 3, 727–748.